



The simple network-based measuring system for improving the evaporation estimation

Dagmar Dlouhá^{1*} , Lukáš Pospíšil¹ , Viktor Dubovský¹ 

¹ VSB – Technical University Ostrava, Faculty of Civil Engineering, Department of Mathematics, Ludvíka Podéště 1875/17, 708 00 Ostrava-Poruba, Czech Republic; dagmar.dlouha@vsb.cz (DD); lukas.pospisil@vsb.cz (LP), viktor.dubovsky@vsb.cz (VB)

*Correspondence: dagmar.dlouha@vsb.cz

Article history

Received 10.05.2023
Accepted 07.08.2023
Available online 11.09.2023

Keywords

evaporation
hydric recultivation
calibration
measuring network
regression

Abstract

This paper presents a novel method for measuring the data for evaporation estimation as the key ingredient for the final decision of the reclamation form in the area of the Most Basin. The area has been intensively mined for many decades, resulting in significant landscape devastation, loss of natural habitats, and negative environmental impact. Currently, it is assumed that by 2050, three large-scale reclamation projects will be implemented in the area and it is necessary to decide which form of reclamation to choose. Whether to build lakes according to the currently valid rehabilitation and reclamation plan or to leave the area of the quarries in succession with the support of spontaneous inflow of water up to a naturally sustainable water level. Whether the first or second option is approved, or a combination of both, the prediction of evaporation from the free water surface will always be of great importance. To deal with this goal, the available meteorological data must be combined with a suitable calculation method. In our work, we suggest utilizing a measuring network of meteorological devices that describe the character of the weather in a given area of interest in a long-term time series. Together with the state-of-the-art calibration of models for calculating evaporation, the measurement network helps to provide more accurate evaporation data for a given area. Based on the analysis of research results, it will be possible to choose a specific right decision and thus contribute to the long-term sustainability of these reclamations.

DOI: 10.30657/pea.2023.29.38

1. Introduction

The history of coal mining in the Most Basin dates back to the 19th century. This area, which is located in the northwestern part of the Czech Republic, is one of the largest lignite basins in Europe and has rich reserves of lignite. The first surface mining activities were started for the requirements of industry and energy in the region. Over time, mining technology and infrastructure in the area developed. During the 20th century, mining methods were expanded and modernized, including the use of large mining machines and belt conveyors to transport coal. Mining in the Most Basin (Fig. 1) was intensive and contributed to the development of the region, but on the other hand, it led to the devastation of the landscape, the loss of original ecosystems, and the creation of coal heaps and surface mines. These mining consequences have a negative impact on biodiversity, air quality, and water resources in the region (Kowol et al., 2020).

During the last decades, brown coal mining in the Most Basin has been reduced under the gradual transition to renewable energy sources and efforts to protect the environment. This led to the closure of some lignite mines and a shift to renewable energy sources such as water power (Grebski et al., 2022), wind power and solar power. At the same time, the process of remediation and restoration of affected areas in the Most Basin is also underway to restore natural habitats, restore soil and water quality, and create recreational and tourist zones. Efforts to protect the environment and the transition to sustainable energy sources are important topics in this field today.

All over the world, there is currently a trend to create so-called "sustainable development", especially when mitigating the impacts of mining activity. That is the reclamation that will be stable in the long term and will enable future generations to further use the reclaimed land.



© 2023 Author(s). This is an open access article licensed under the Creative Commons Attribution (CC BY) License (<https://creativecommons.org/licenses/by/4.0/>).

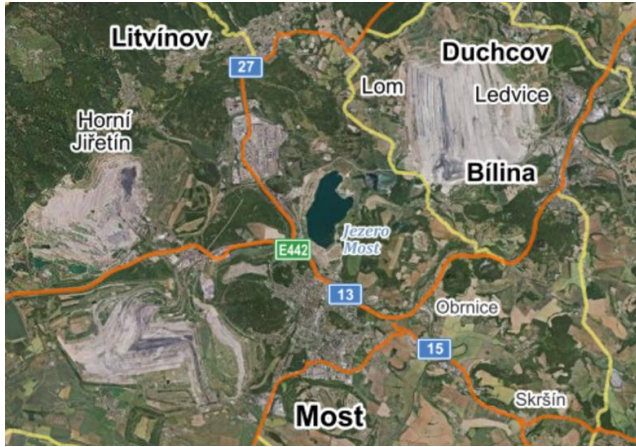


Fig. 1. The map of the area of interest: surface brown coal mines in the Most Basin (source: www.mapy.cz)

Now it is necessary to decide what form of recultivation to choose. Whether to build lakes according to the currently valid plan of reclamation and recultivation or to leave the quarry area to succession with the support of natural water inflow until the naturally sustainable water level is reached. Whether the first or the second option is approved, or a combination of both, the prediction of evaporation from the open water surface will always be of great importance.

When determining the potential evaporation from the open water surface in the Most Basin area, we can utilize the fact that hydraulic recultivation of the Ležáky-Most quarry has already been carried out in this region. Before the initiation of flooding the residual pit, a series of remediation measures were necessary. These included sealing the bottom of the future lake, constructing an underground sealing wall, and building fortifications along the shoreline. All of these described measures, combined with the fact that Lake Most has no natural inflow or outflow, allow us to view Lake Most as a closed isolated area. Lake Most has become a “laboratory” for us, where we can verify the results of our work and subsequently apply the same procedures in planned recultivation areas.

Evaporation from the open water surface is a process in which water molecules evaporate from the surface of the water into the surrounding air. The water molecules overcome the forces of attraction and acquire sufficient kinetic energy to transition into a gaseous state. This process is influenced by factors such as air temperature, air humidity, air pressure, air velocity above the water surface, solar radiation intensity, and the surface area of the water. Evaporation can be measured using evaporation pans or evaporation gauges on water bodies. However, this process is costly and complex. Even so, it can be subject to errors due to external influences (e.g., waves on the water), and thus cannot be considered as a standard. Therefore, there are various computational methods available to estimate the magnitude of evaporation. This multitude of methods led the Food and Agriculture Organization of the United Nations (FAO) to determine the most suitable or at least a reference method that could be used in a broad range of investigated cases. In (Allen, 1998), FAO recommended the Penman-Monteith equation in the following form as the standard method for calculating potential evapotranspiration.

$$E_{FAO} = \frac{0.408\Delta(R_n - G) + \gamma \frac{900}{T_a + 273} u_2 (e_s - e_a)}{\Delta + \gamma(1 + 0.34u_2)} \quad (1)$$

In the formula, E_{FAO} denotes the intensity of evapotranspiration in $mm d^{-1}$ and it is calculated using the following variables and constants: the symbol Δ represents the slope of the saturation vapor pressure curve at a given air temperature, R_n is the net radiation at the surface, and G is the change in heat storage in the soil or water; R_n and G are expressed in $MJ m^{-2} d^{-1}$. According to the article by Linacre (Linacre, 1993), for daily or monthly estimates of open water evaporation rates, G can be neglected by setting $G = 0$. The expression $(e_s - e_a)$ in kPa represents the difference between the saturation vapor pressure and the actual vapor pressure, while u_2 denotes the wind speed at a height of $2 m$ above the surface in ms^{-1} . The constant γ depends on the atmospheric pressure P in kPa , and T_a is the air temperature in $^{\circ}C$.

From a long-term series of climatic data, it is evident that the average annual air temperature during the period of 2014-2018 increased by approximately $2^{\circ}C$ compared to the period of 1970-2013. As a result, the evaporation from the open water surface is approximately 6% higher (Fig. 2). Considering precipitation and air temperature scenarios for the future period and assessing the impact of climate change scenarios on the hydrological balance of the pilot area make the simulating and predicting the future hydrological balance of the studied area an essential part of the preparation for the planned hydraulic recultivation. Only through these means can the expected evaporation from the open water surface be estimated and utilized to establish a long-term sustainable water balance in the studied area (Dlouhá et al., 2021b).

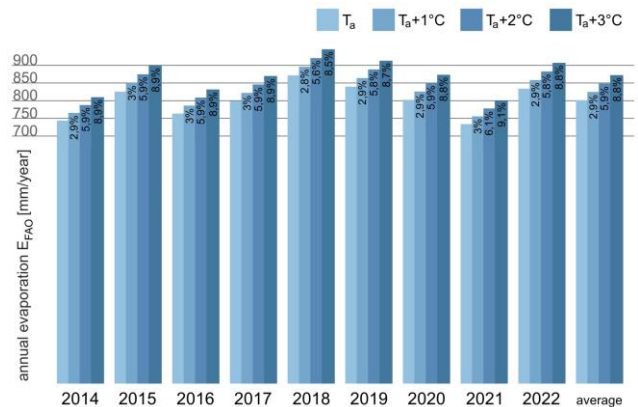


Fig. 2. The percentage increase in annual evaporation computed using E_{FAO} caused by increased air temperature T_a

Each region has the specific conditions, which can vary even within the same area of interest. The reason why it is important to have well-measured climate data in a sufficiently long time series is illustrated by the graph (Fig. 2) depicting the percentage increase in annual evaporation sums computed using E_{FAO} (1) if the average air temperature were to increase by $1^{\circ}C$, $2^{\circ}C$, or $3^{\circ}C$.

Additionally, as it is necessary to work with a continuous series of measurements, there is a risk of data loss in the event of a point source failure.

These reasons have led to the idea of establishing a network of meteorological micro-stations covering the area of interest.

2. Literature review

The complex issue of evaporation is addressed in work (Trenberth et al., 2011). The FAO equation (1) is a solid standard but sometimes too complex to be practically handled. For example, the paper (Jabloun et al., 2008) studies eighteen temperature, radiation, mass, and combined methods under climate change conditions in Germany. The FAO equation (Allen et al., 1998) is compared with 31 methods under humid climatic conditions in Iran in article (Gavilán et al., 2007). Five temperature methods and three radiation methods are considered in (Lovelli et al., 2005; Dlouhá et al., 2021a, b).

In our previous work, we have studied long-term series of climate data in our area of interest and weather forecast predictions (Dlouhá et al., 2021c).

The paper (Dubovský et al., 2022) deals with the issue of developing and equipping a network of meteorological micro-stations considering acceptable measurement inaccuracies and costs.

From a large number of combined methods for calculating evaporation, we have selected the Hargreaves-Samani equation as the most suitable for our calibration, as introduced by Hargreaves in article (Hargreaves, 1975) and further modified and described in (Hargreaves et al., 1985).

The calibration of models using different statistical measurements and cross-validation technique is addressed in articles (Dlouhá et al., 2021a; Stone, 2011; R Core Team. R. 2013; Gay, 1990). Statistical measurements are described in (Mohawesh, 2011; Mostafa et al., 2012; Djaman et al., 2016; Lang et al., 2008; Yao, 2009; Cabrera et al., 2016; Moriasi et al., 2007).

The existing literature primarily relies on analyses that are based on data obtained from a single location. However, our research holds significant importance in the field as it addresses the critical issue of evaporation from a large lake, necessitating the utilization of measured values from multiple locations to ensure a comprehensive understanding of the area of interest. This paper presents a novel and valuable methodology that significantly contributes to the advancement of knowledge in this particular research domain.

3. Experimental

The problem of establishing a monitoring network for the collection of hydrometeorological data can be divided into several following fundamental steps:

- analysis of the area (field survey, spatial analysis in GIS),
- analysis of data requirements (precipitation, air temperature, wind speed and direction, streamflow, groundwater levels, etc.),

- analysis of data availability in the area of interest and its vicinity,
- initial design of the monitoring network and data interpolation in GIS (Thiessen, Kriging, etc.),
- operation of the monitoring network, including the production of data inputs for hydrological modeling,
- optimization of the monitoring network.

3.1. Testing area

The testing area became Lake Most. Since April 2017, the creation and installation of a network of meteorological micro-stations on Lake Most (Fig. 3) and its immediate surroundings began. The measured values are transmitted using a Wi-Fi network.

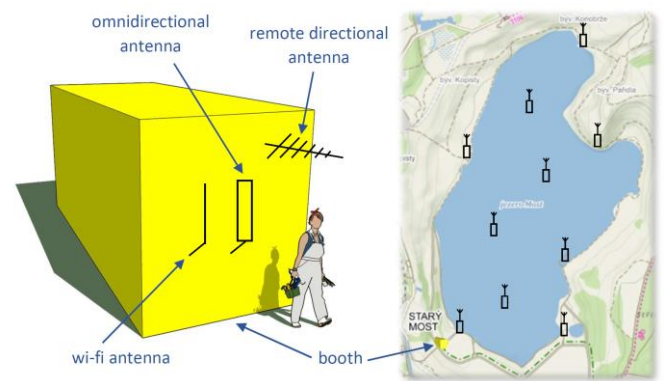


Fig. 3. Schematic network diagram

Due to the special conditions of placing the meteorological micro-stations and the necessity to transmit measurement results using a radio signal to the central station located in the guard building of Lake Most, the most suitable and cost-effective solution was chosen; stations have been equipped with a radio module for data transmission through an internal radio network (Fig. 4). The meteorological micro-stations are equipped with sensors to measure air temperature, water temperature at the surface and at a depth of 1 meter, relative humidity, and air pressure (Fig. 5 and Fig. 6). However, the temperature of the water at the surface and at depth does not directly enter the formulas for calculating evaporation. Therefore, it is not necessary to measure it for evaporation calculations.

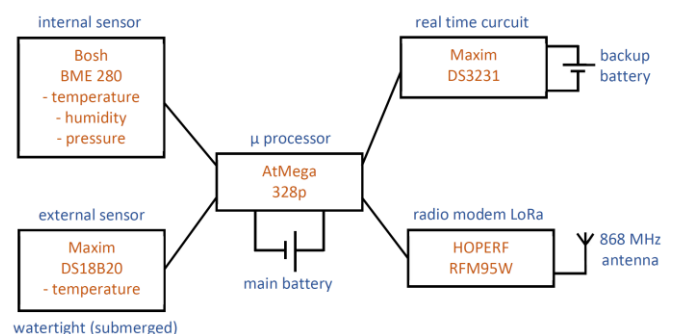


Fig. 4. Schematic diagram of a meteorological micro-station

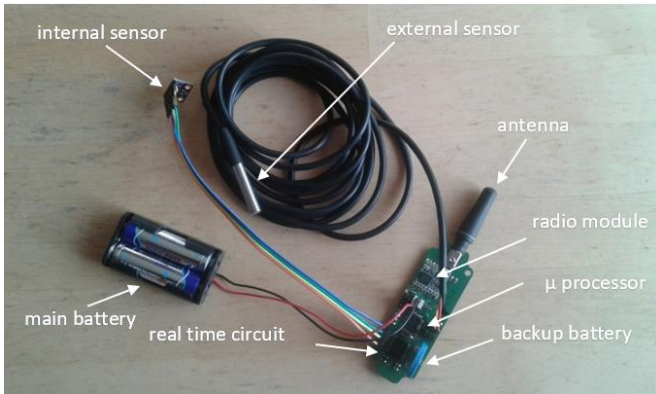


Fig. 5. The meteorological micro-station



Fig. 6. The meteorological micro-station is placed in a protective casing and in a radiation shield

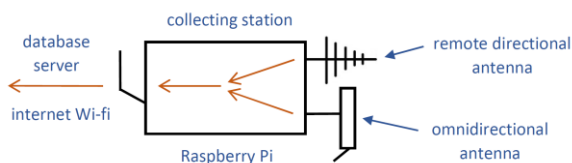


Fig. 7. Schematic diagram of a collection station

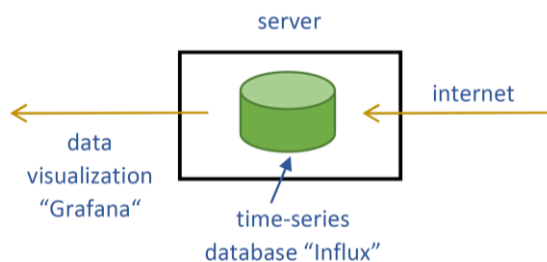


Fig. 8. Schematic diagram of measurement processing

Data measurements are conducted at minute intervals and can be monitored online and further processed (Fig. 7), (Fig. 8). We use the Grafana software for our work (Fig. 9). As a means of energy saving, it is possible to transmit data for processing, for example, once every ten minutes.

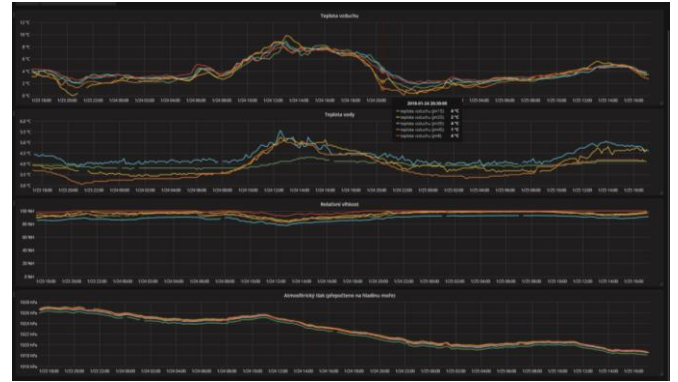


Fig. 9. Grafana software

The use of a measurement network leads to improved estimates of evaporation and subsequently to a better model of lake surface evaporation behavior, for which Thiessen polygons have been employed. By using Thiessen polygons, the lake can be divided into sub-areas. The Thiessen polygon method was selected from a range of data interpolation methods from the station network as the most suitable because the area of interest for each planned hydrological reclamation project involves an extent where the z-coordinate can be disregarded, and the problem can be addressed in a planar setting.

Thiessen polygons (also known as Voronoi polygons, Dirichlet regions, proximity zones, Wigner-Seitz cells) define individual influence areas around each measurement point. The assembly of Thiessen polygons begins with a suitable triangulation in a vector model, which involves constructing a corresponding triangular network over the measurement points. For example, Delaunay triangulation is commonly used, based on the principle that no other point should fall within the circum-circle of each triangle. Subsequently, the sides of the triangles are bisected by perpendicular lines, which define the boundaries of the Thiessen polygons. In a bitmap image of the area, the construction is even simpler because it only requires assigning the value of the nearest known pixel to each polygon.

Thiessen polygons can be used to predict values at corresponding surrounding area from a single measurement point, serving as a simple interpolation method. However, the method has several limitations:

- The division of the area into Thiessen polygons is entirely dependent on the observation locations. This creates polygons that do not correspond in shape to the phenomenon being mapped. For example, long and narrow polygons are created, or polygons at the edge of the area theoretically have infinite area. In practice, this issue is addressed by clipping (using the "Clip" function) in GIS using watershed lines or other boundaries of the area of interest.
- The value within each polygon is derived from a single sampling point (usually a point of measurement), which means that the accuracy of the method depends on the ratio of the area size to the number of polygons.
- The interpolation error cannot be calculated.

- There is no assumption of spatial correlation between the measurement values (autocorrelation), meaning that nearby locations are not expected to have more correlated values than more distant locations.

The size of the sub-regions is naturally determined by the number of stations (i.e., number of measurement points) and the suitability of their distribution. Another undeniable advantage of having a larger number of stations is their representativeness and reliability. If one of them fails, the lost data can be replaced by data from neighboring stations or the subdivision into sub-regions can be adjusted.

In case of station failure, there is a redistribution of polygons; see the difference between Fig. 10 and Fig. 11, where the number of stations changed due to the failure of one station.



Fig. 10. Subdivision into subregions for five stations

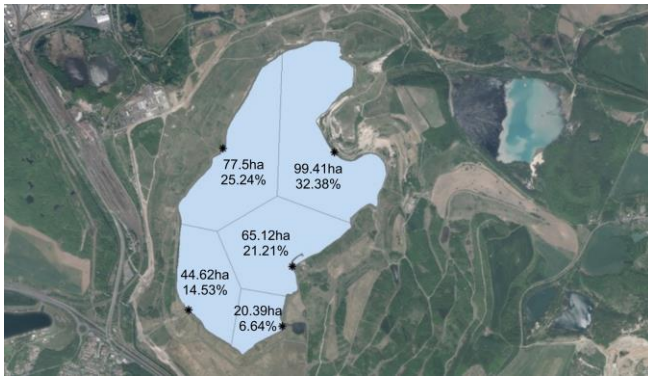


Fig. 11. Subdivision into subregions for four stations

The number of stations depends on the phase of the reclamation planning and the availability of suitable locations for their safe placement. The minimum number of stations should be at least four, which will remain stationary throughout the measurement period. These fixed stations can be supplemented with portable stations that capture changes in the characteristics of the observed area, thus providing additional potential locations for measurements.

The design of the stations also depends on the type of model which will be used to calculate the evaporation. If potential evaporation is determined solely based on temperature equations, then measuring only air temperature is sufficient. However, if it is determined using a combined equation, it is necessary to measure not only air temperature but also pressure,

humidity, wind speed, sunshine duration, and global radiation. Global radiation can be either calculated or measured using a pyranometer, which is sufficient to be measured at only one station. In addition to the variables required for the calculation of potential evaporation, it is also advisable to measure precipitation at the stations.

Considering our experience with signal outages, it is recommended to equip the stations, or at least the central collection station, with the capability to back up measured data.

3.2. Calibration of temperature models

One of the key components of planning hydrological reclamation is securing long-term sustainability, which is based on the ability to maintain a stable water level. Therefore, it is necessary to know the potential evaporation in the area of interest. The recommended Penman-Monteith equation E_{FAO} (1) is demanding in terms of input data and calculations. For this reason, we searched for a simplified evaporation model for the Most Lake area. Several simplified models for evaporation estimation were selected and compared from literature, and their coefficients were subsequently calibrated to achieve the highest possible agreement with the results of the Penman-Monteith equation E_{FAO} (1). In this case, statistical measures such as the Nash-Sutcliffe efficiency coefficient NSE (2), root mean square error $RMSE$ (3), mean absolute error MAE (4), and percent bias $pbias$ (5) were used as comparative criteria.

$$NSE(E_{FAO}, E) = 1 - \left[\frac{\sum_{t=1}^T (E_{FAO}(t) - E(t))^2}{\sum_{t=1}^T (E_{FAO}(t) - \bar{E}_{FAO})^2} \right] \quad (2)$$

$$RMSE(E_{FAO}, E) = \sqrt{\sum_{t=1}^T (E(t) - E_{FAO}(t))^2} \quad (3)$$

$$MAE(E_{FAO}, E) = \frac{1}{T} \sum_{t=1}^T |E(t) - E_{FAO}(t)| \quad (4)$$

$$pbias(E_{FAO}, E) = 100 \frac{\sum_{t=1}^T E(t) - E_{FAO}(t)}{\sum_{t=1}^T E_{FAO}(t)} \quad (5)$$

In the previous equations, the term $E(t)$ denotes the model value in time (day) $t = 1, \dots, T$.

The presented statistical measures were used for calibrating model parameters, i.e., for each model and measure, we solve the corresponding regression minimization problem

$$\theta^* = \arg \min \rho(E_{FAO}, E(\theta)) \quad (6)$$

in the case of measures $\rho \in \{RMSE, MAE, PBIAS\}$ given by equations (3)-(5), or the regression maximization problem

$$\theta^* = \arg \max \rho(E_{FAO}, E(\theta)) \quad (7)$$

in the case of $\rho = NSE$ given by (2). In both problems, $E(\theta)$ represents the considered parametric model that needs to be calibrated. During the experiments with model calibration using various statistical measures, it was observed and mathematically proven that maximizing NSE and minimizing $RMSE$ yield the same optimum.

To avoid overfitting of the calibrated models, a cross-validation method (Stone, 2011) was adopted. The data were randomly divided into calibration and validation subsets. The model parameters were optimized on the calibration set and tested on the validation set. The results from the validation set were further analyzed, and the best model was selected based on the results from all cross-validation splits.

4. Results and discussion

4.1. The measurement network at Lake Most

Let us briefly discuss our experiences with long-term measurements in the area of Lake Most. There are differences in the measured air temperatures at individual stations (Fig. 12). Station 51 serves as a reference and is located outside the influence area of the lake. Stations 15, 25, 36, and 45 are located along the lakeshore, while stations 8, 11, 21, 31, and 41 are positioned at the lake surface.

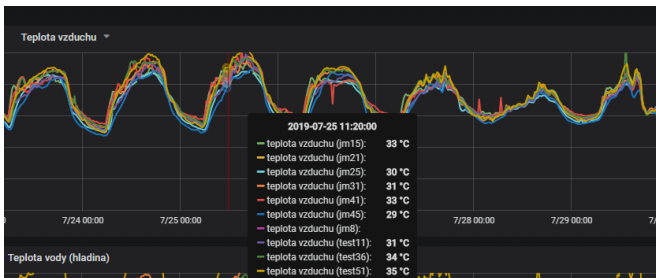


Fig. 12. Grafana software - air temperature measurements

Differences are also evident in the measured values of relative humidity (Fig. 13).

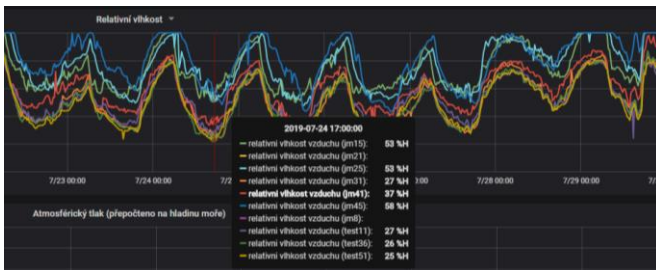


Fig. 13. Grafana software – relative humidity

On the contrary, the measured values of sea-level adjusted atmospheric pressure consistently show similar values over the long term. Any small deviations have a negligible impact on the value of evaporation (Fig. 14).

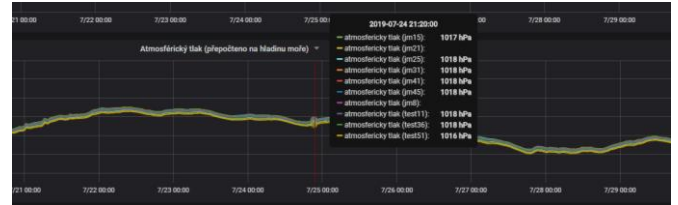


Fig. 14. Grafana software – air pressure measurements

The data from the network was processed for each corresponding polygon. In these defined areas, the evaporation E_{FAO} was calculated. The sum of evaporation in individual polygons is compared to E_{FAO} , which was calculated using data from the Kopisty meteorological station. For example, the graph (Fig. 15) depicts the annual variation from December 2017 to November 2018.

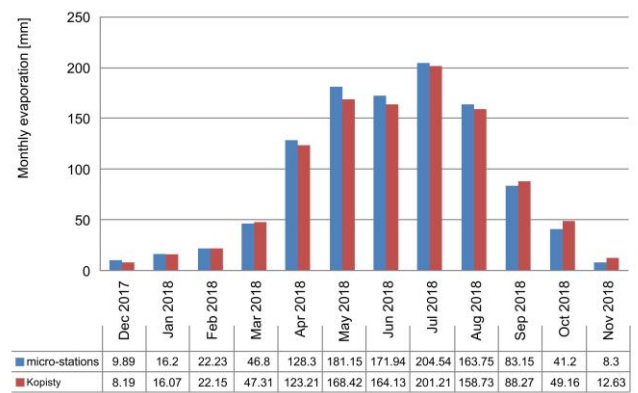


Fig. 15. Comparison of monthly evaporation E_{FAO} between the network and the Kopisty meteorological station

Afterwards, the data corresponding to these defined sub-regions is related to the respective meteorological micro-stations, allowing more accurate modeling of the behavior of Most Lake and, above all, a more accurate estimation of evaporation.

4.2. Calibration of the Hargreaves-Samani equation

From our previous results, the most suitable simple model for evaporation estimation is the Hargreaves-Samani equation. This equation is usually presented in the form

$$E_{HS} = 0.0023 \frac{R_a}{\lambda} (T_a + 17.8) \sqrt{T_r} \quad (8)$$

where T_a denotes the average air temperature ($^{\circ}\text{C}$), T_r is the difference between the maximum and minimum air temperature during the observed period ($^{\circ}\text{C}$), the value of specific heat capacity of water $\lambda = 2,45\text{MJkg}^{-1}$, and R_a refers to extraterrestrial radiation. Although Equation (8) includes the radiation term R_a , the model is classified as a temperature equation. The reason is that this expression only represents the theoretical value of radiation, which is calculated based on the latitude of the considered area φ and the solar declination δ determined

by the day number in the year. The value E_{HS} provides results in millimeters per day.

The corresponding parametric form of the Hargreaves-Samani equation can be written as

$$E_{HS}(\theta) = \max \left\{ 0, \frac{\theta_1 R_a (T_a + \theta_2) \sqrt{T_r}}{\lambda} \right\} \quad (9)$$

with parameters $\theta \in \mathbf{R}^2$. These parameters were optimized during the calibration process. The maximum is used to avoid negative evaporation value.

The calibration process was implemented in the R programming language (R Core Team. R., 2013). This software provides an easy way to load and manipulate data, solve optimization problems using in-built optimization algorithms, and present results in the graphical form. The type of optimization problem depends on the considered model and the selected statistical criterion, see (6) and (7). Several optimization algorithms available in the R programming language were compared in terms of computational time and result accuracy. Based on the comparison, the *nlm* algorithm from the *optim* package was found to be the most efficient option for solving the presented optimization problems. This algorithm utilizes the *PORT* routines (Gavián, 1990). The performed numerical experiments demonstrated its suitability, robustness, and stability in solving linear and nonlinear models.

In order to generalize the calibration process, the K-fold cross-validation method was used (Stone, 2011). Modeling with a random subset of data generalizes the results and prevents overfitting. Ten random permutations of the data were performed, and each permutation was divided into 10 parts - 9 parts were used for model calibration, and the remaining part was used for validation. This permutation process was repeated 100 times, and for each of these permutations, 10 calibration-validation splits were performed. In total, 1000 results of the calibration process were obtained and analyzed.

Calibration and validation were performed with respect to all the aforementioned statistical measures. Due to the best fit of the model to the values calculated according to the Penman-Monteith equation FAO, it was selected as the most suitable equation

$$E_{HS}^{NSE} = 0.0021 \frac{R_a}{\lambda} (T_a + 17.5571) \sqrt{T_r} \quad (10)$$

The equation was obtained through calibration performed with respect to NSE. Fig. 16 provides a comparison of monthly evaporation calculated using the FAO Penman-Monteith equation (1), the Hargreaves-Samani equation (8), and the calibrated Hargreaves-Samani equation (10) in the form of a cumulative sum and a scatter plot.

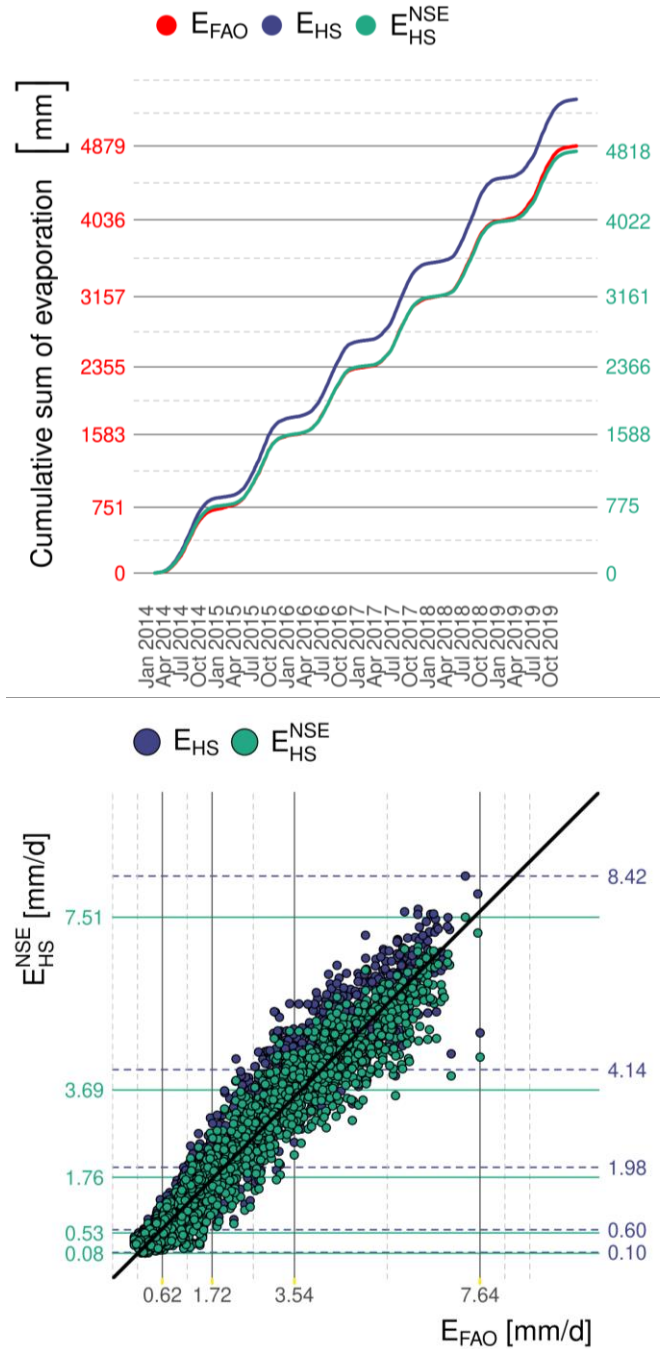


Fig. 16. Comparison of daily evaporation calculated using the FAO Penman-Monteith equation, Hargreaves-Samani equation, and calibrated Hargreaves-Samani equation with respect to NSE in the form of cumulative evaporation (top) and a scatter plot (bottom). The data used in both images are from January 2014 to October 2019

The results obtained from the six-year time series indicate that the calibrated Hargreaves-Samani model (10) seems to be the most suitable simplification of the FAO Penman-Monteith equation in the area of Lake Most. This equation demonstrated sufficient approximation to the FAO Penman-Monteith equation and additionally requires only temperature as input, which can be easily (and inexpensively) measured by meteorological micro-stations.

5. Summary and actual work

The measurement and calibration processes that we have verified at Lake Most are now being utilized for estimating potential evaporation from the water surface, which will eventually be located in the ČSA quarry area. In this area of interest, three professional weather stations Albrechtice, Marcela, and OM (Obránci) have already been installed there and measurements at these stations recorded at 30-minute intervals will serve as a basic input to our models.

Since April 2022, we have started the development and installation of a network of meteorological micro-stations at the ČSA quarry, which will complement these professional stations. Currently, two micro weather stations are equipped with sensors for measuring air temperature, relative humidity, and air pressure. Measurement locations were selected at an elevation of 180 meters above sea level, designated as ZS 2 and DS 2 (Fig. 17). Currently, preparations are underway for the installation of ten additional micro-stations that will cover the ČSA quarry area.

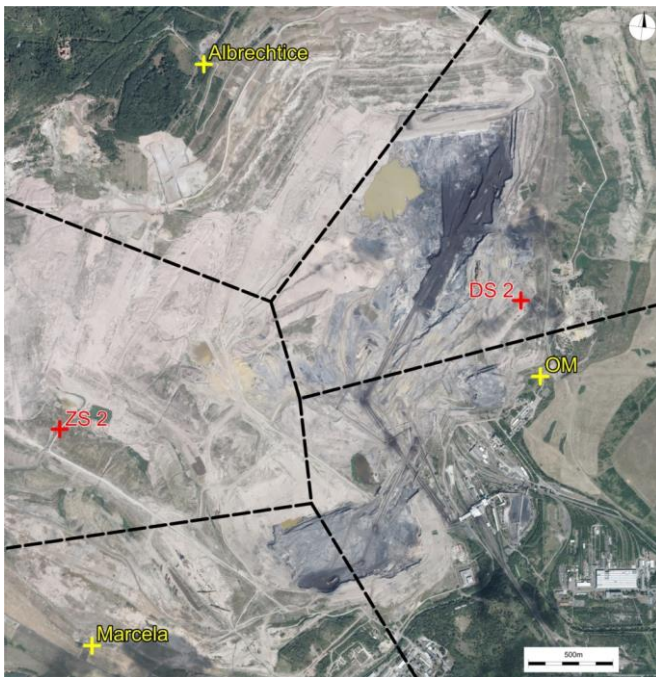


Fig. 17. Locations of all stations in the ČSA quarry area

The area of approximately 6.5 km² with a water level of 180 meters above sea level, as one of the options for the planned quarry reclamation, has been divided and assessed using Thiessen polygons to determine proportions and areas for each variant (Fig. 18). From the initial results, it is evident from the graph (Fig. 19) that it is not suitable to rely on a single data source when planning reclamation projects. The differences in evaporation rates from different stations are significant.

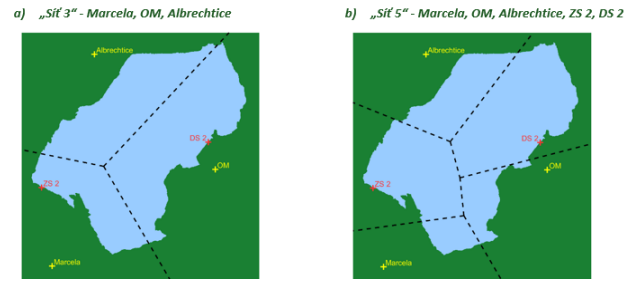


Fig. 18. Division into sub-regions of ČSA quarry area

The obtained results demonstrate the adaptability of the proposed methodology, which can be applied effectively across varying numbers of stations. This flexibility accommodates scenarios wherein the number of stations may fluctuate over time, such as the addition of new stations or temporary station failures. In all cases, it is evident that an increased number of stations yields enhanced coverage of the designated area. Future research endeavors incorporating a greater number of microstations will enable a thorough analysis of the correlation between the quantity of measuring devices and the resultant quality of estimated evaporation. This exploration will provide valuable insights into the relationship between station density and the accuracy of evaporation estimations, contributing to further advancements in the field.

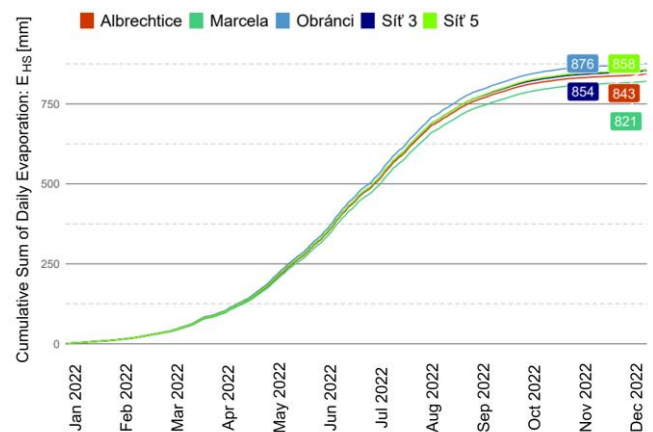


Fig. 19. Cumulative evaporation sums E_{HS} : individual professional stations, network of professional stations, and the entire network, year 2022

6. Conclusion

In conclusion, this paper has outlined a methodology for estimating the evaporation rates of existing and future planned lakes in the Most Basin. The central element of this approach is the utilization of a network of meteorological microstations, which provides a more comprehensive coverage of the area of interest compared to relying solely on a single professional meteorological station. By employing this method, more accurate and localized estimations of evaporation can be obtained, thus enhancing our understanding of water balance dynamics in the region. This research contributes to the field by offering a practical and effective solution for estimating

evaporation in large lake systems, with potential applications in water resource management and planning for sustainable development. We hope that our work will contribute to refining the evaporation from the free water surface and thus to maintaining a sustainable water balance in the area of the planned recultivation after brown coal mining.

Acknowledgements

We would like to express our gratitude to Ing. Václav Přibík, who implemented the measurement network at Most Lake and at the ČSA quarry. We would also like to thank the company Diamo, the administrator of Most Lake, and the company Seven, the owner of the ČSA quarry, for their collaboration and material assistance. This contribution was made possible thanks to the funding provided by our Department of Mathematics at FAST, VŠB-TUO.

Reference

- Allen, R.G., Pereira, L., Raes, D., Smith, M., 1998. Crop evapotranspiration - Guidelines for computing crop water requirements - FAO. Irrigation and drainage paper, 56, United Nation - Food and Agriculture organisation.
- Cabrera, M., Anache, J., Youton, C., Wendland, E., 2016. Performance of evaporation estimation methods compared with standard 20 m² tank. *Rev. Bras. Eng. AgriCola Ambient*, 20, 874.
- Djaman, K., Balde, A., Sow, A., Muller, B., Irmak, S., N'Diaye, M., Manneh, B., Moukoubi, Y.D., Futakuchi, K., Saito, K., 2015. Evaluation of sixteen reference evapotranspiration methods under sahelian conditions in the Senegal River Valley. *Journal of Hydrology: Regional Studies*, 3, 139–159.
- Dlouhá, D., Dubovský, V., Pospíšil, L., 2021. Optimal Calibration of Evaporation Models against Penman–Monteith Equation. *Water*, 13(11), DOI: 10.3390/w13111484.
- Dlouhá, D., Dubovský, V., Pospíšil, L., 2021. The Evaporation Estimation on Lake Most. *MAPE*, 4(1), 221–231, DOI: 10.2478/mape-2021-0020.
- Dlouhá, D., Dubovský, V., 2021. Specification of the Climate Character in the Study Area of Projected Hydric Reclamation. *Inžynieria Mineralna*, 47(1), 75–79, DOI: 10.29227/IM-2021-01-10.
- Dubovský, V., Dlouhá, D., Jarošová, M., 2022. On the Influence of the Measurement Inaccuracy on the E_{FAO} Evaporation Estimates (in the Area of the Lake Most). *AIP Conference Proceedings*, DOI: 10.1063/5.0081483.
- Gavilán, P., Berengena, J., Allen, R.G., 2007. Measuring versus estimating net radiation and soil heat flux: Impact on Penman–Monteith reference ET estimates in semiarid regions. *Agricultural Water Management*, 89, 275–286.
- Gay, D.M., 1990. Usage summary for selected optimization routines. *Computing Science Technical Report No. 153*, 1–21.
- Grebski, W., Grebski, M., 2022. Project of Micro-hydroelectric Power Generation, System – Case study. *Production Engineering Archives*, 28(2), 178–184, DOI: 10.30657/pea.2022.28.21.
- Hargreaves, G., 1975. Moisture Availability and Crop Production. *Transactions of the ASAE*, 18, 0980–0984. DOI: 10.13031/2013.36722.
- Hargreaves, G., Samani, Z., 1985. Reference Crop Evapotranspiration From Temperature. *Applied Engineering in Agriculture*, 1. DOI: 10.13031/2013.26773.
- Jabloun, M., Sahli, A., 2008. Evaluation of FAO-56 methodology for estimating reference evapotranspiration using limited climatic data: Application to Tunisia. *Agricultural Water Management*, 95, 707–715.
- Kowol, D., Kurama, H., 2020. Recovery of Fine Coal Grains from Post-Mining Wastes with Use of Autogenous Suspending Bed Technology. *Management Systems in Production Engineering*, 28(4), 220–227, DOI: 10.2478/mspe-2020-0032.
- Lang, D., Jiangkun, Z., Shi, J., Liao, F., Ma, X., Wang, W., Chen, X., Zhang, M., 2017. A Comparative Study of Potential Evapotranspiration Estimation by Eight Methods with FAO Penman–Monteith Method in Southwestern China. *Water*, 9, 734.
- Linacre, E.T., 1993. Data-sparse estimation of lake evaporation, using a simplified Penman equation. *Agricultural and Forest Meteorology*, 64, 237 – 256, DOI: 10.1016/0168-1923(93)90031-C.
- Lovelli, S., Piza, S., Caponio, T., Rivelli, A., Perniola, M., 2005. Lysimetric determination of muskmelon crop coefficients cultivated under plastic mulches. *Agricultural Water Management*, 72, 147–159.
- Mohawesh, O., 2011. Evaluation of evapotranspiration models for estimating daily reference evapotranspiration in arid and semiarid environments. *Plant Soil Environ*, 57, 145–152.
- Moriasi, D., Arnold, J., Van Liew, M., Bingner, R., Harmel, R., Veith, T.L., 2007. Model evaluation guidelines for systematic quantification of accuracy in watershed simulations. *Transactions of the ASABE*, 50, 885–900.
- Mostafa, A., Benzaghta, M. Benzaghta, A., Mohammed, A., Ekhmaj, A., 2012. Prediction of Evaporation from Algardabiya Reservoir. *Libyan Agriculture Research Center Journal International*, 3, 120–128.
- R Core Team R., 2013. *A Language and Environment for Statistical Computing*. R Foundation for Statistical Computing, Vienna, Austria.
- Stone, M., 1974. Cross-validatory choice and assessment of statistical predictions. *Journal of the Royal Statistical Society: Series B (Methodological)*, 36, 111–147.
- Trenberth, K.E., Fasullo, J.T., Mackaro, J., 2011. Atmospheric Moisture Transports from Ocean to Land and Global Energy Flows in Reanalyses. *Journal of Climate*, 24, 4907–4924, DOI: 10.1175/2011JCLI4171.1.
- Yao, H., 2009. Long-Term Study of Lake Evaporation and Evaluation of Seven Estimation Methods: Results from Dickie Lake, South-Central Ontario, Canada. *Journal Water Resource and Protection*, 2, 59–77, DOI: 10.4236/jwarp.2009.12010.

用于改进蒸发估计的简单的基于网络的测量系统

關鍵詞

蒸发
水分复垦
校准
测量网络
回归

摘要

本文提出了一种测量蒸发量数据的新方法，作为最终决定大盆地地区填海造地形式的关键因素。该地区几十年来一直被密集开采，造成了严重的景观破坏、自然栖息地的丧失和对环境的负面影响。目前，预计到 2050 年，该地区将实施 3 个大型填海项目，需要决定选择哪种填海形式。是根据当前有效的恢复和围垦计划建造湖泊，还是在水自流入的支持下连续离开采石场区域，直至达到自然可持续的水位。无论第一个或第二个选项被批准，还是两者的组合，自由水面蒸发的预测总是非常重要的。为了实现这一目标，必须将可用的气象数据与合适的计算方法相结合。在我们的工作中，我们建议利用气象设备的测量网络来描述长时间序列中给定感兴趣区域的天气特征。与用于计算蒸发的最先进的校准模型一起，测量网络有助于为给定区域提供更准确的蒸发数据。根据研究结果的分析，将有可能选择具体的正确决策，从而有助于这些填海工程的长期可持续性。